

Investigating the Mechanics of Human-Centered Soft Robotic Actuators with Finite Element Analysis

Keith W. Buffinton, Benjamin B. Wheatley, Soheil Habibian, Joon Shin, Brielle H. Cenci, and
Amanda E. Christy

Abstract— Increasing attention has been focused in recent years on the development and analysis of “soft” robots. Such tools can perform a variety of simple tasks in and around humans with minimal risk of injury to people and the environments in which people typically live and work. Some studies have developed computational models, such as finite element models, to compare to experimental analysis. While these models generally show strong agreement with experiments, there has been little use of models to investigate modeling assumptions, buckling behavior, or design spaces. This paper seeks to address these opportunities and challenges through finite element analysis (FEA) of a particular type of soft actuators known as Fiber Reinforced Elastomeric Enclosures (FREEs), both individually and in modules. The FREEs studied in this work are fabricated from thin-walled latex tubes with helically wound cotton fibers at particular angles relative to the tube. Our results suggest that elastomer material behavior can be better described with an Ogden rather than neo-Hookean material model at large deformations and by modeling fibers with 1D truss elements. Additionally, the material properties of the elastomer were found to greatly influence FREE extension, expansion, and rotation (with strains in excess of 25%), while changes to fiber stiffness resulted in negligible differences in deformation. The implications of these results are that in the design and manufacturing of FREEs, substantial attention must be given to accurately measuring, modeling, and understanding elastomer and adhesive properties, and that these may be used for design tuning. Additional results showed that modules made up of multiple FREEs can be effectively studied using FEA to determine range of motion, buckling, and workspace.

I. INTRODUCTION

One of the challenges in the design of robots for use in and around humans is that robots are typically made structurally stiff to ensure precise movements and adequate structural strength. Unfortunately, the use of structurally stiff robots in proximity to humans increases the risk of injury to the humans as well as the environments in which they typically live and work. As a result, robotic researchers have recently focused on the development of “soft” robots that can perform a variety of simple tasks. Contact-friendly soft robots can not only better interact with their spatial environments but also better maneuver in confined spaces. Schultz [1] describes the situation more broadly, and highlights the importance of soft

robotics in future technology and where we stand in its current technological development:

It will not be long until affordable, reliable, easy-to-use robots are able to help us directly in many ways... Soft robots (autonomous agents where significant material deformation is an integral part of the robot’s function) have an important role to play in this bright robot-enabled future. Soft robotics is a field that is moving out of its infancy and into adolescence [1].

One promising type of soft robot actuator is a Fiber Reinforced Elastomeric Enclosure (FREE). FREEs represent a subset of the types of pneumatically controlled compliant structures currently being studied by a number of researchers [2-8]. These fluid-controlled actuators are inherently soft and able to apply various forces and torques while deforming freely (specifically in extension, expansion, or rotation) when used either singly or in serial or parallel combinations. The major design component of interest in a FREE is generally regarded as the helically wound fibers that surround an elastomeric cylinder and are adhered to this substrate. Indeed, much work has been performed investigating the effect of various families of fibers, fiber number, and fiber orientation (see for example [3,4]). Elastomeric material, however, has a variety of ways that its behavior may be described mathematically beyond the neo-Hookean [3,9] and Mooney-Rivlin [10] constitutive equations. Relatively little attention has been given to how this model choice is best made, and it remains unclear how elastomer structural and material properties affect FREE function. Moreover, to our knowledge, there have been no previous analyses of buckling behavior of FREEs, such as those presented here.

Previous studies have considered analytical models of FREE motion [4] and force [5,9] generation based on fiber geometry, and continuum methods have been used to capture the inherent nonlinearity of FREEs in relating kinematic behavior to torsional loading [6]. Finite element analysis (FEA) of FREEs presents a robust approach to studying a broad scope of FREE behavior through prompt simulations in comparison to repeated experimentation. However, there exists limited finite element investigations of FREE behavior [3,4], and in particular there is a distinct lack of use of FEA as a tool to extrapolate beyond experimental studies, including

K. W. Buffinton is a Professor of Mechanical Engineering (corresponding author; phone: 570-577-1581; e-mail: keith.buffinton@bucknell.edu).

B. B. Wheatley is an Assistant Professor of Mechanical Engineering (e-mail: b.wheatley@bucknell.edu).

S. Habibian is a graduate student in Mechanical Engineering (e-mail: s.habibian@bucknell.edu).

J. Shin is an undergraduate in Mechanical Engineering (e-mail: js118@bucknell.edu).

B. H. Cenci is a graduate student in the Johns Hopkins Center for Bioengineering Innovation and Design (e-mail: bhc003@bucknell.edu).

A. E. Christy is an undergraduate in Electrical & Computer Engineering (e-mail: amanda.christy@bucknell.edu).

All authors, unless otherwise noted, are either faculty or students at Bucknell University, Lewisburg, PA 17837 USA.

buckling behavior. The goal of this work is to develop and implement a robust finite element model of individual and modular FREE actuators and to use this model to optimize the design of soft robotic manipulators.

The specific topics investigated in this paper include material selection of the elastomer and fiber, with a particular emphasis on how elastomer mechanics influences FREE mechanics; fiber orientation and FREE deformation; element selection for FREE fibers, the effect of adhesives on FREE deformation, and FREE module deformation. We aim to answer the following questions 1) how do these modeling assumptions and procedures affect simulated FREE behavior, 2) how can we use these simulations to drive future soft robotics design, and 3) what is the modeling workspace of modules made of multiple FREEs?

In the following sections, we develop detailed analyses of these considerations beginning in Section II with a detailed description of our FREE model formulation. In Section III, we present results that corroborate those in [3] as well demonstrate the validity of our own model. New results and observations of the behavior of a single FREE are given in Section IV, and Section V presents results not previously achieved by others for a module of four FREEs. Concluding remarks are presented in Section VI highlighting the most significant results of our work as well as limitations and planned future directions of investigation.

II. FREE MODEL FORMULATION

Fiber Reinforced Elastomeric Enclosures (FREEs) consist primarily of two components, an elastomer and a fiber, and thus represent a composite material. The elastomer has the role of the matrix of material supporting the fibers, which provide additional resistance to loads. FREEs can be used as pneumatic actuators in mechanical systems by applying a pressure to their internal surface. In effect the elastomer acts to transfer fluid pressure (generally a compressible gas) into fiber axial stress and thus whole FREE deformation. There are a variety of parameters that affect such an actuator's response, including both geometric and material properties. The choice of these parameters in designing FREEs is determined by the desired application and overall response characteristics, but is not fully understood.

Finite element analysis (FEA) has previously been used to study the effect of various fiber orientations on FREE mechanics [3,4]. FEA is used here to develop a detailed model (Abaqus, Dassault Systèmes) of an elastomeric tube wound at a specified angle by a thin fiber. Model geometry includes three regions: a deformable three-dimensional elastomeric tube, rigid end caps, and deformable fibers wound at the same angle on the exterior of the tube, as shown in Fig. 1A.

To investigate material properties and FREE behavior, various constitutive models were considered for the elastomer. These included a linear elastic and two different hyperelastic models, neo-Hookean and first-order Ogden. Fibers were modeled as linear elastic. Contact and adhesion between elastomer and fibers was modeled with tied conditions. Pressurization of a FREE results in three distinct deformations: extension, expansion, and rotation as shown in Fig. 1B. All models were run in Abaqus/Standard with the proximal cap

face pinned and pressure applied to the elastomer interior surface.

III. CALIBRATION AND VALIDATION

To determine material properties for the model, three separate experimental investigations were conducted. First, the true stress-strain relationship for the latex elastomer was obtained through both uniaxial material testing in an Instron 5965 with a dogbone sample and through axial stretching of an elastomeric tube. The resulting linear curve fit (1.18 MPa) provides a Young's Modulus for further model development. The elastomer was assumed to be incompressible ($\nu=0.5$). A further check that the data were in a reasonable range was done by calculating the elastic modulus corresponding to typical Shore A hardness numbers for latex (35 ± 5 [11]). An elastic modulus of 1.18 MPa corresponds to a Shore hardness of 30.8 based on the formula given in [12], which is within the expected range.

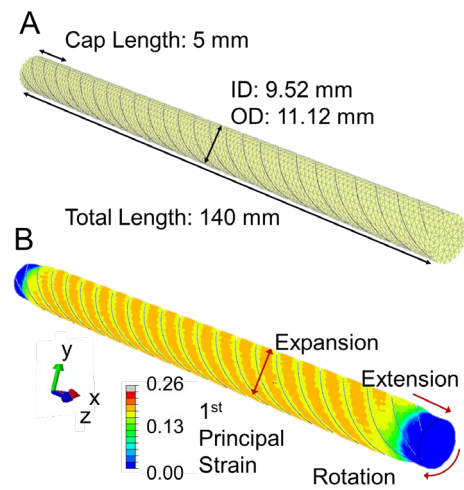


Figure 1. A) FREE finite element model highlighting mesh density, elastomer dimensions, and fiber geometry. B) FREE deformation at 60 kPa internal pressure. Contour plot shows 1st principal logarithmic strain.

Similar experiments were performed for cotton fibers to determine the tensile force-strain relationship. Load-strain data were acquired to provide the relationship between fiber strain and the product of modulus and cross-sectional area of the fiber (EA). This enabled the use of truss elements for cotton fibers in the finite element model. Fitting the linear region of the test results gave a value of structural stiffness equal to $644 \text{ N}/\epsilon$. As shown later in this paper, the exact value of EA is in fact not critical to the analysis due to the significantly greater stiffness of the cotton fibers relative to the latex elastomer.

Once the material and structural properties of the constituents were determined, the effect of fiber-elastomer adhesive (rubber cement) on the overall structural response was investigated. In short, we conducted additional expansion tests using a simple latex tube without a fiber winding and then applied *only* adhesive and a thin latex coating *without* a fiber winding to gauge their impact on the overall stiffness of the tube. The tubes each had a 9.52 mm (3/8") inside diameter, 0.8 mm (1/32") wall thickness, approximately 130 mm tube length, and 5 mm caps on each end. Measurements were taken as pressure within the tubes was increased from 0 to 3.5 psi

(corresponding to strains comparable to those experienced in similar fiber-wound FREEs pressurized up to 10 psi).

Figure 2 shows the experimentally determined expansion ratios measured with the uncoated tube and then measured with the same tube after adhesive and a thin latex coating was applied. As can be seen, the coated tube is stiffer in expansion than when uncoated (expansion is reduced with increasing pressure, Fig.2). Finite element simulations of this experiment led us to investigate material models other than neo-Hookean, which becomes too soft at high pressures (Fig. 2). We specifically explored the use of a first-order Ogden hyperelastic model (Equation 1, where λ_i are the principal stretches, μ is the shear modulus of the material, and α is a material constant).

$$\Psi(\lambda_1, \lambda_2, \lambda_3) = \frac{2\mu}{\alpha} (\lambda_1^\alpha + \lambda_2^\alpha + \lambda_3^\alpha - 3) \quad (1)$$

Use of an Ogden model requires the determination of the initial shear modulus μ as well as the material parameter α that characterizes nonlinearity. Based on the previously determined elastomer modulus and the diverging of coated and uncoated tube expansion at higher pressures (Fig. 2), we chose to fix our initial shear modulus at 0.393 MPa (converted from $E=1.18$ MPa and $\nu=0.5$) and vary α through a sensitivity study. Figure 2 shows expansion ratio curves for values of α from 0.8 to 2 (note that with $\alpha = 2$, the Ogden model reduces to the neo-Hookean model). By calculating the root-mean-square error between models and data shown in Fig. 2, an Ogden model with $\alpha = 1.2$ was determined to be the best representation of the behavior of a coated FREE (RSME with $\alpha = 1.2$ was 50% less than with $\alpha = 0.8$ and 85% less than with $\alpha = 2$). Note that the use of other elastomer materials would likely yield other values of α but were not considered in the present work.

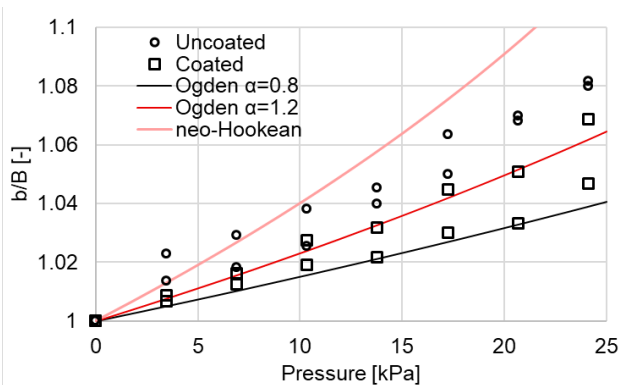


Figure 2. Radial expansion ratio measured on uncoated and coated latex tubes as well as predicted using an Ogden material model ($\alpha = 0.8$ to 2). Open markers denote experimental data and solid curves denote predictions.

Model validation was conducted on experimental data of FREE rotation data using the geometry, assumptions, and material properties described above. Figure 3 displays curves characterizing the rotation of a latex elastomer FREE with fiber winding angles of 20°, 50°, and 70° as predicted by our calibrated FEA model. Also plotted are experimentally determined data points for three FREEs with the same winding angles, inside diameter 9.52 mm (3/8”), wall thickness 0.8 mm (1/32”), and 130 mm length. These data and simulation results show that our model has strong predictive capability across various fiber angles pressurizations. Agreement between predicted and measured results reinforce our confidence in our

calibration method and our general approach to modeling the behavior of the FREEs. We were able to use the model built from tensile and expansion (Fig. 2) data (elastomer $\mu=0.393$ MPa and $\alpha=1.2$, fiber $EA=644$ N/ε) to accurately predict FREE rotation (Fig. 3). We chose rotation for validation as it is the principal deformation of interest for most FREEs. Specifically, large rotations of individual FREEs can be used to design coordinated bending and translation of FREE modules.

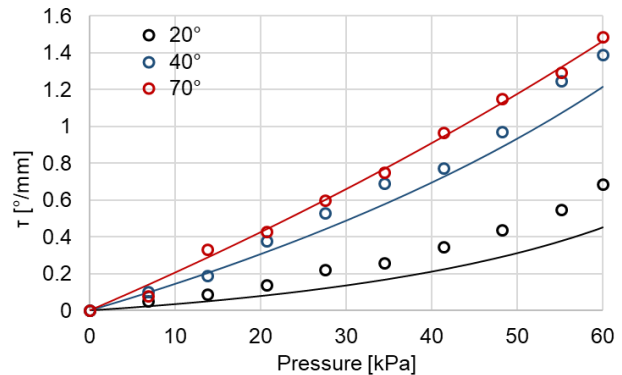


Figure 3. FEA rotation validation showing twist per unit length in $^\circ/\text{mm}$ as a function of pressure for fiber angles of 20°, 50°, and 70° as well as corresponding experimental data points. Open circles denote experimental data points and curves denote model predictions.

IV. INVESTIGATIVE RESULTS

A. Variations in Fiber Winding Angle

Other researchers [3,4] have used FEA to study the behavior of fiber-reinforced soft fluidic actuators with an emphasis on fiber organization. Reference [3] provides particularly relevant comparative data as we used the same modeling framework to develop our geometry and mesh. See [3] for full details of their system parameters and methodology. We chose to explore the three FREE deformations (extension, expansion, and rotation) of our model similar to the work in [3] to provide further confidence in our approach. As can be seen in Fig. 4, cases are considered with fiber angles ranging from 10° to 80°. As the fiber angle is increased, the radial expansion (b/B) increases and the axial extension (λ_z) decreases until expansion is a maximum and extension is zero at a fiber angle of 90°. As pointed out in [3], noteworthy results are that the extension is non-monotonic (i.e., the length of the FREE decreases) for fiber angles in the range of 50° to 80° and that the angle of twist per unit length (τ) reaches a maximum at a fiber angle of approximately 30°.

In considering the non-monotonic increase in length described in the preceding paragraph, note that the theoretical winding angle at which a filament wound pressure vessel reverses direction between elongation and contraction is 54.7° [13]. While this theoretical result is not strictly applicable to a FREE consisting of a soft elastomer wound by a single family of fibers (i.e., all fibers are wound at the same angle) and in which the properties of the elastomer play an important role, our finite element model observed a similar transition from elongation to contraction between 60° and 45°.

While the material properties used here differ significantly from those used in [3], similar trends were observed. Thus, we have confidence in our modeling approach to explore various design considerations as outlined in the following sections. These similarities in trends also suggest that the following

characteristics are similar for all FREE-like actuators: 1) a specific fiber angle at which extension transitions from negative to positive, 2) increasing expansion as fibers align with actuator length, and 3) a fiber angle at which rotation is maximum for a given pressure.

B. Fiber Element Type

Previous finite element modeling of FREEs have used second-order, one dimensional beam elements to model the reinforcing fibers based on the expectation that the bending stiffness of Kevlar fibers contributes to the overall response [3]. While beam elements are more likely to produce a stable solution when used in a nonlinear finite element model, there is concern over the use of an element type that supports bending loads for the cotton fibers used here. Physically, the bending loads capable of being supported by the cotton fibers used to fabricate our FREEs are negligible in relation to the internal FREE pressure and axial loads supported by the fibers. Thus, we chose to implement second-order “truss” elements, capable of supporting only axial loads.

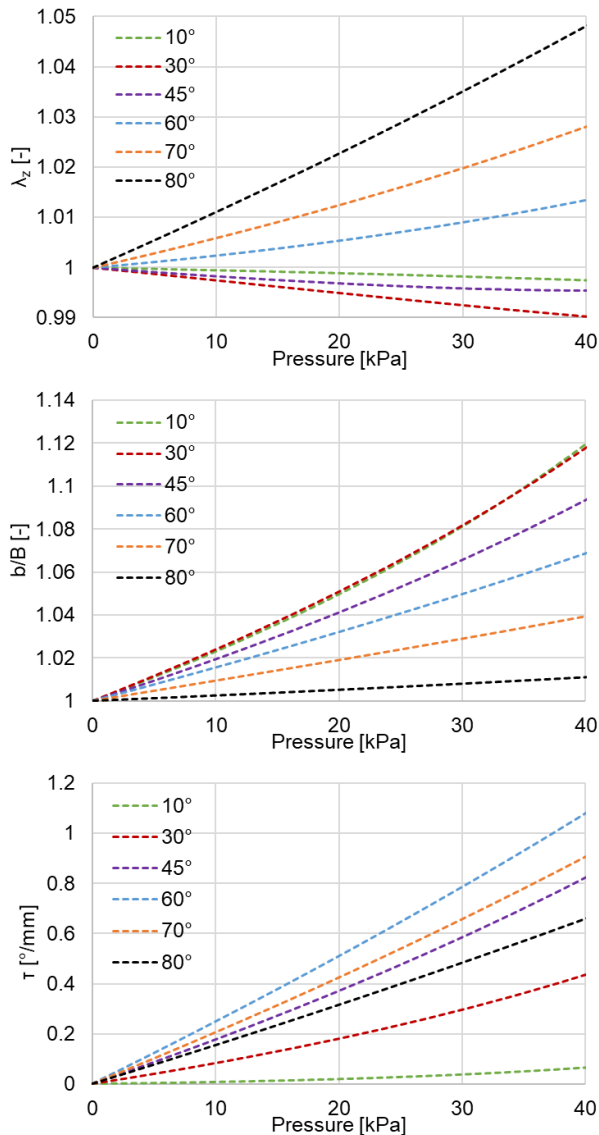


Figure 4. FEA of FREEs for fiber angles over the range of 10° to 80° showing extension (λ_z), expansion (b/B), and rotation per length (τ) as a function of applied pressure.

The effect of truss versus beam elements is not evident during individual FREE pressurization, as the fibers are subject primarily to axial loads as a result of the internal pressure applied to the elastomer. However, deformations that could cause FREE bending or buckling are likely to exhibit significantly different model results based on fiber element type. This is seen by imposing an axial extension on the FREE model with zero applied internal pressure and comparing structure deformation for beam versus truss elements (Fig. 5).

The observed buckling with truss elements (Fig. 5A) and a lack of buckling with beam elements (Fig. 5B) suggests that modeling FREE behavior with truss fibers more closely simulates experimental behavior for our system, as FREEs often buckle when subject to non-pressurized deformations (see [9] for experimental buckling behavior). The assumption of beam versus truss also has significant implications in modeling modules made up of multiple FREEs, where bending or buckling is likely to occur (see section V). Thus, we recommend future models use truss elements for fiber materials that do not support significant bending loads.

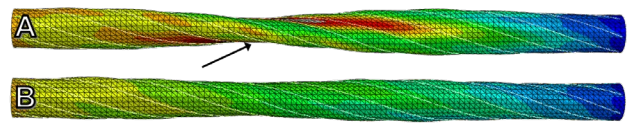


Figure 5. FEA deformation color contour map for an axial extension of 2 mm comparing fiber A) truss elements and B) beam elements. The truss elements show FREE buckling (shown with arrow) that is consistent with experimental observations.

C. Elastomer Material Properties

As shown in Fig. 2, our implementation of an Ogden hyperelastic model enabled a better fit to experimental expansion data in comparison to a neo-Hookean model. This is due to the softening behavior of a neo-Hookean model as finite strains increase [14]. In comparison, an Ogden model (Eq. 1) enables the user to define a shear modulus μ and a nonlinear coefficient α . For elastomeric pressurized vessels, the nonlinearity and specific constitutive model is of great importance due to “snap buckling”. A physical example of this is the observation that at some pressure during the inflation of a balloon, expansion becomes easier as pressure increases. From a finite element perspective, this can cause significant convergence issues as the tangent stiffness can become approximately zero or even negative, thus preventing convergence in a static analysis.

To overcome what we believe to be this difficulty, previous investigations [3] generated the desired internal pressure through thermal expansion to achieve convergence at large fiber angles (80° and up). This thermal expansion enforces a volume constraint on the FREE interior, making the analysis deformation-driven in comparison to the load-driven analysis used here. However, we did not observe these convergence issues when using an Ogden model for the elastomer. This is likely due to the fact that the Ogden model does not soften at higher pressures like the neo-Hookean model, and prevents snap buckling for the deformations observed in this study.

Thus, we are confident in our choice to implement a first-order Ogden model in this work. However, as previously discussed, prior finite element investigations of FREE kinematics have largely focused on fiber alignment and

number [3,4], and have neglected to fully investigate the effect of elastomer material properties. Thus, we chose to employ a parametric study of FREE behavior using a 20° fiber winding angle as a baseline. This winding angle yields significant extension and rotation as compared to other winding angles, which makes this winding angle particularly well suited for FREE-driven robotic devices.

As Fig. 6 shows, variations in elastomer material properties can greatly influence FREE behavior. Due to elastomer strains in excess of 25% (see Fig. 1B), significant changes in elastomer stiffness can greatly affect deformation. In fact, halving the Ogden shear modulus of the elastomer more than doubled FREE extension, expansion, and rotation. If one considers the deformation of greatest interest to be rotation, then the sizeable increase in rotation with decreased modulus is a significant effect in the context of FREE design.

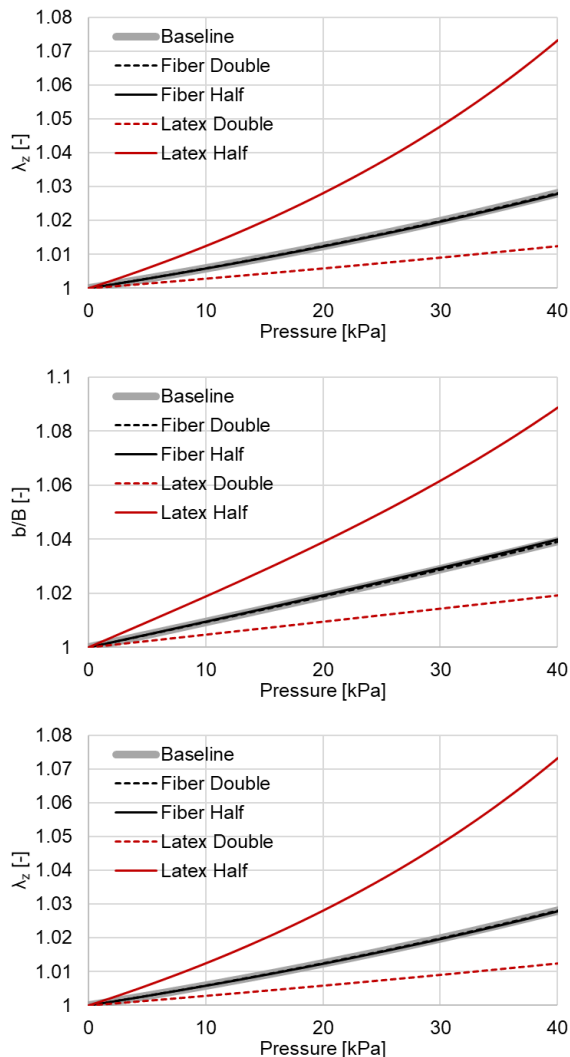


Figure 6. FEA of FREEs with doubling and halving of elastomer and fiber material properties for a fiber angle of 20° showing extension (λ_z), expansion (b/B), and rotation/length (τ) as a function of pressure.

Just as relevant is the effect of adhesive coatings (Fig. 2) on whole FREE behavior. While the main purpose of these adhesives is to attach stiff reinforcing fibers to the soft elastomer, this layer of material also can itself affect FREE

response. Thus, for design and manufacturing purposes, the thickness of adhesive layers and type of adhesive should be carefully considered. Based on these observations, we suggest carefully considering the following regarding FREE design and manufacturing, in addition to fiber number and winding angle, as they are likely to play a role in FREE mechanics:

1. Elastomer thickness and material properties
2. Adhesive thickness and cured material properties

The implication of these results when designing and manufacturing FREEs is that careful attention must be given to accurately measuring, modeling, and understanding elastomer properties. A failure to do so may result in significant differences between desired performance of a FREE and observed behavior. The same holds true for the adhesive, as great care should be taken to ensure the thickness of the adhesive coating is controlled. We suggest that this adhesive may contribute to FREE mechanics in a greater sense than simply adhering the fibers to the elastomer.

Alternatively, this phenomenon could be used to expand the design space of FREEs, in particular adding an additional design parameter or parameters (elastomer and adhesive properties) to alter FREE behavior (Fig. 7). Here we can see that halving the material properties of latex for a 70° winding angle more than doubles the rotation per unit length. This approximately doubles the range of rotation when compared to Fig. 4. Variations in fiber winding angle produce a maximum rotation per unit length at approximately 60°, as increasing and decreasing angles both reduce rotation (Fig. 4). The relationship between rotation and elastomer stiffness does not exhibit this maximum, as decreases in elastomer modulus continue to increase rotation. However, we can see that at low fiber angles and low elastomer stiffness, the rotation-pressure relationship becomes highly nonlinear. This suggests real-world control of a FREE in this case may be extremely difficult due to small pressure fluctuations resulting in relatively high rotations. Thus, while varying elastomer and adhesive properties can expand the design space of FREEs, one must ensure it does not come at the cost of FREE control.

From a manufacturing perspective, this could enable FREE mechanics “tuning” by varying adhesive thickness or by using different elastomer materials. This could be particularly advantageous for FREE applications that require specific design considerations such as lightweight components, high control accuracy, or low cost. Overall, most important is still that elastomer and adhesive structural properties are properly understood and carefully monitored for optimal FREE control.

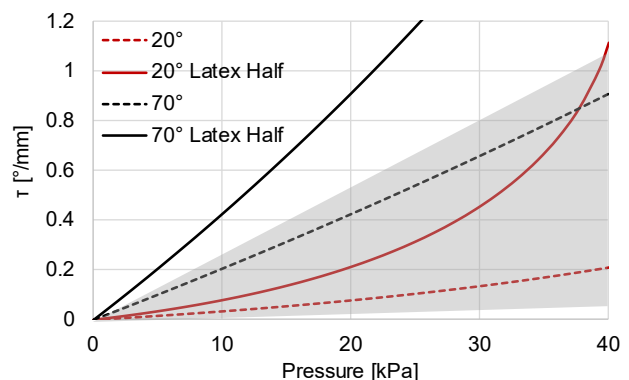


Figure 7. Rotation/length of FEA simulations comparing baseline (dashed) and halved (solid) elastomer material properties. The gray shaded region represents the space covered by varying fiber angle from Fig. 5, while the red curve show fiber angles of 20° and the black curves show fiber angles of 70°. By including variations in elastomer material properties, one can see that this greatly expands the design space of FREEs.

D. Fiber Material Properties

As shown in Fig. 6, changing the stiffness of the fibers has little effect on FREE extension, expansion, or rotation. Because the fiber deformation is so small relative to the elastomer, the exact fiber stiffness appears to have little effect on overall behavior so long as the fibers are significantly stiffer than the elastomer. While there is certainly a point at which decreased fiber stiffness will begin to impact FREE behavior, this is unlikely to be a challenge in the design, manufacturing, and control of FREEs operating under similar conditions.

V. MODULE OF MULTIPLE FREEs

A single FREE is not sufficient to create a soft robotic arm that is expected to perform various maneuvers in a three dimensional space. An arrangement of FREEs in a module, however, has the potential to produce novel motions and forces and to create the performance characteristics of a full robotic arm. There are various geometric arrangements for every distinct combination of FREEs in a module and thus experimentally investing all the possible combinations to develop a soft robotic arm would be extremely tedious. As an alternative, in this section a finite element model of a square-module of four FREEs has been generated for FREEs with winding angles of 30°, 40°, and 60°. In all cases tested, FREEs are modeled with a length of 175 mm, an inner diameter of 9.52 mm, a wall thickness of 0.8 mm, and wound with six fibers each. An illustration of a pressurized four-FREE module is shown in Fig. 8. In this case, each of the four FREEs have a clockwise 40° winding angle and two diagonally opposed FREEs (shown in green) have been pressurized to 7.25 psi.

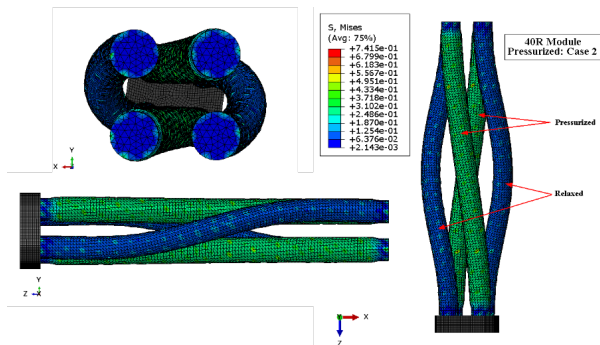


Figure 8. Module consisting of four FREEs with clockwise winding angles of 40° and two diagonally opposed FREEs pressurized to 7.25 psi.

Fiber winding direction is important in the design of a module. The fibers can be wound in either a clockwise (R) or counterclockwise (L) direction which correspondingly determines the direction of rotation of the FREE. We use the naming convention that “R” and “L” modules have all clockwise or all counterclockwise winding angles, respectively, with a module combining one pair of each winding direction (two L and two R, each diagonally across from one another) denoted as “LR”.

Models of four modules with winding angles and winding directions of 30° (LR), 60° (LR), 40° (LR), and 40° (R) were created and tested over a range of pressures. For each module, five different cases were identified to explore the relationship between module pressurization and displacement. The convention of numbered cases is shown in Fig. 9 that displays which of the FREEs numbered (1, 2, 3, and 4) is pressurized for each case.



Figure 9. Convention indicating FREEs pressurized in each case.

Results suggest that cases 1, 2, and 4 are the most fundamentally useful in creating particular motions. Having all of the FREEs pressurized (case 1) in an LR-module produces pure elongation [Fig. 10(a)]. Case 2 produces rotation without bending in an LR-module [Fig. 10(b)]. And pressurizing two adjacent FREEs (case 4) causes the module to deform in pure bending [Fig. 10(c)].

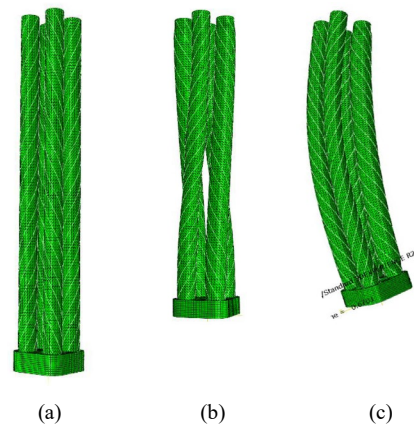


Figure 10. Model of a 30° RL-module showing deformations for (a) case 1, (b) case 2, and (c) case 4.

An important consideration in the design of any robotic manipulator is the range of reachable locations, i.e., its workspace. Workspace is determined by geometry and kinematic design. In the case of a single FREE, the workspace is simply a one dimensional line. Creating a module of multiple FREEs allows the attainment of a volume of points. To explore the reachable workspace of a module, the model of a 60° LR-module was run for each of the five pressurization cases defined in Fig. 9 and the position of the free end of the module was mapped in space.

Figure 11 shows that cases 1 and 2 generate a one dimensional line (as expected) while cases 3, 4, and 5 result in paths generated through bending and twisting of the module. The set of reachable points form a concave shaped workspace. Note that although each case has its own unique set of orientations within the workspace, only reachable *locations* are studied in this analysis. As can be seen in Fig. 11, the pure bending produced by Case 4 results in straight line projections of the paths in the X-Y plane that extend approximately 36 mm from the origin. The bending and twisting of Cases 3 and 5 result in curved projections in the X-Y plane that extend approximately 25 mm from the origin (note that the studies represented in Fig. 11 are limited to 7.25

psi; higher pressure would result in a larger workspace). Overall, these results give an indication of the boundaries of the workspace and provide insight into the kinematic capabilities of the 60° LR-module. Similar results can be produced for other module configurations and a desired kinematic design selected for a given application. However, these simulations require further experimental validation before these results can be useful in designing and manufacturing FREE modules.

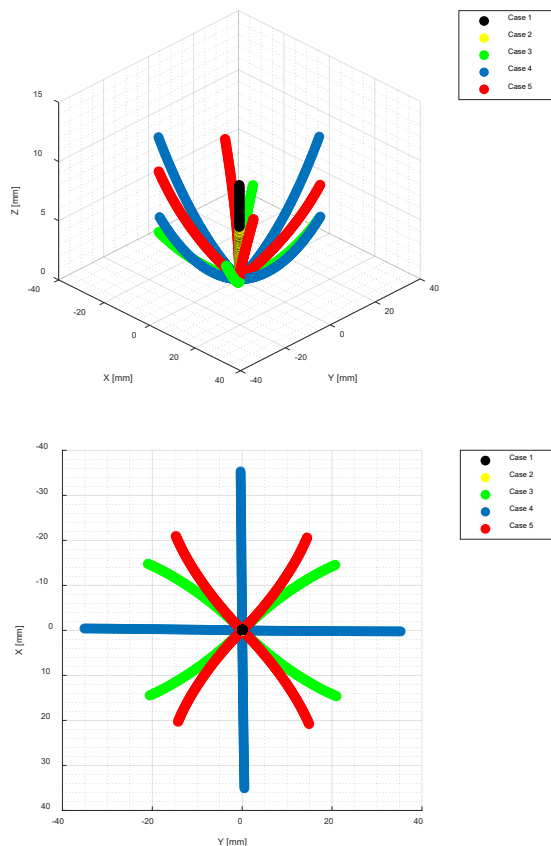


Figure 11. Two views of the reachable points for a 60° LR-module. The top view shows the paths taken by the tip of the module as the FREEs are pressurized from 0 to 7.25 psi for each of Cases 1 through 6. The bottom view shows the corresponding projections of the paths in the X-Y plane.

To continue the exploration of the 60° LR-module's workspace, combinations of pressurizations for Cases 3 through 5 were used to determine reachable points between the lines shown in Fig. 11. Linear interpolation was then used to estimate workspace boundaries and Figure 12 depicts this estimate. The figure clearly shows the points that are potentially reached as the pressure within the FREEs is increased from 0 to 7.25 psi.

As mentioned in section IV, a common issue observed in the behavior of FREEs is buckling. Although an overall pattern of buckling in modules is difficult to establish, large amounts of twist, particularly at low pressures, can often result in buckling. Figure 13 illustrates the buckling behavior of the 60° LR-module in pressurization Case 2. As can be seen, the two diagonally opposed, non-pressurized FREEs have buckled (note that a small positive pressure in the FREEs significantly decreases the likelihood of buckling). As a

result, guaranteeing that all points in the interior of volumetric workspace are in fact reachable may not be possible due to potential buckling in particular cases. Finite element analysis nonetheless provides a useful tool in identifying the reachable points within the workspace, aiding designers in evaluating various configurations of FREEs before manufacturing.

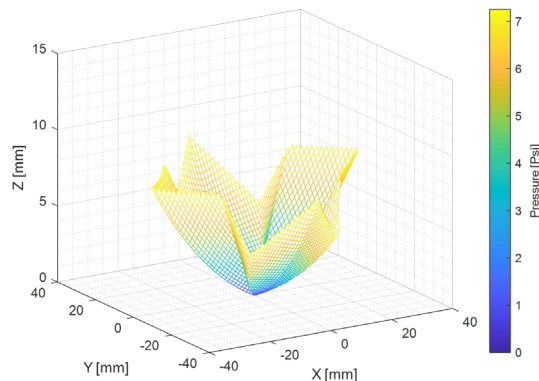


Figure 12. Linearly interpolated estimate of workspace for a 60° LR-module

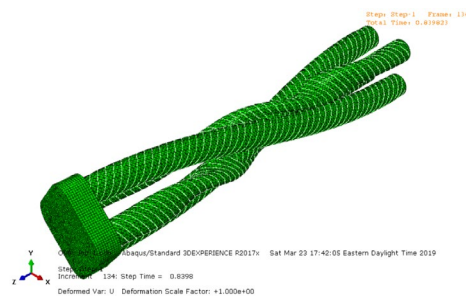


Figure 13. Buckling of the 60° LR-module pressured to 7.25 psi

VI. CONCLUSION

We have formulated a detailed finite element model of a fiber reinforced elastomeric enclosure (FREE) using previously validated geometric approaches [3]. This model investigated, and later suggested, the use of an Ogden model to characterize the hyperelastic behavior of the elastomer in comparison to a commonly used neo-Hookean approach. We calibrated our model with experimentally measured material properties of both latex elastomer and cotton fibers, and further explored elastomer and adhesive structural properties by measuring FREE expansion. The validation by comparing computational and experimental rotation data for FREEs of various fiber winding angles and at increasing pressures demonstrated the efficacy of our approach. Thus, our model was calibrated based on relevant manufacturing attributes and validated for the deformation of greatest interest (rotation) when FREEs are used as actuators in robotic arms. Moreover, we have extended our analysis to include kinematic descriptions of workspaces generated by modules of multiple FREEs as well as buckling behavior of both individual and modules of FREEs, results which have not been reported by others. Simulations of multiple FREEs require further validation, however, before these results can influence the design and implementation of FREEs in human-robot interactions.

While the results presented here provide a variety of new insights under a range of conditions, there are nonetheless extensions of our work that could consider additional factors affecting FREE behavior. These include, for example, the consideration of external loads, the use of multiple families of fiber angles in a single FREE (or module), and a more in-depth evaluation of FREE extension and expansion, rather than focusing primarily on rotation. More broadly, one could consider a statistical constitutive model such as Arruda-Boyce, which may be more accurate for polymers, or an analysis that goes beyond static behavior and includes mass characteristics and dynamic response. Dynamic response in particular is currently being studied and will be the subject of a later paper.

We recommend that future computational analyses of FREEs utilize hyperelastic constitutive models for the elastomer that prevent significant softening at high strains, and that fibers should be modeled with 1D truss elements that only support axial loads. Specifically, bending and/or buckling is almost certain to occur in FREE modules, and typical FREE fibers are unlikely to support bending loads. Parametric analyses show that FREE behavior is highly sensitive to elastomer material properties but relatively insensitive to fiber stiffness. The fiber essentially acts as an inextensible material, relative to the elastomer, once the fiber stiffness exceeds a certain level (additional theoretical analyses related to this observation are given in [15]). The implications of elastomer properties affecting FREE extension, expansion, and rotation are that these must be closely controlled during manufacturing to ensure consistent FREE behavior, or that these could potentially be used to increase the design space of FREEs. Another important future area of study is greater exploration of the force generation of FREE modules. To this end, the novel *force zonotope* methodology developed in [7] is likely to be of considerable value in calculating the generalized forces produced by soft actuators as a function of their internal pressure. The force zonotope can then be used to inform the design and control of parallel combinations of soft actuators.

Overall, we have demonstrated the effectiveness of an Ogden-based finite element approach in predicting the behavior of single and multiple FREEs, with particular attention to developing a greater understanding of the design space of FREEs for use in and around humans. Future single FREE models will focus on detailed studies of the interactions between fiber and elastomer and adhesive thickness. Simulations of modules of multiple FREEs will continue to be investigated to expedite future designs of these systems for interactions with humans, such as providing eldercare.

ACKNOWLEDGMENT

The authors would like to gratefully acknowledge the collaborative support of Prof. C. David Remy, Dan Bruder, and Audrey Sedal of the University of Michigan. They provided the impetus for our work as well as many thoughtful comments and refinements of our ideas. The authors also acknowledge the valuable insights provided by Prof. Christine Buffinton of Bucknell University in determining stress-strain relationships for nonlinear materials as well as corroborating finite element analyses. Finally, Toyota Research Institute (“TRI”) provided funds to assist the

authors with their research but this article solely reflects the opinions and conclusions of its authors and not TRI or any other Toyota entity.

REFERENCES

- [1] J. Schultz, Y. Mengüç, M. Tolley, and B. Vanderborght, “What is the Path Ahead for Soft Robotics,” *Soft Robotics*, vol. 3, no. 4, pp. 159-160, 2016.
- [2] A. D. Marchese, R. K. Katzschmann, and D. Rus, “A Recipe for Soft Fluidic Elastomer Robots,” *Soft Robotics*, vol. 2, no. 1, pp. 7-25, 2015.
- [3] F. Connolly, P. Polygerinos, C. J. Walsh, and K. Bertoldi, “Mechanical Programming of Soft Actuators by Varying Fiber Angle,” *Soft Robotics*, vol. 2, no. 1, pp. 26-32, 2015.
- [4] G. Krishnan, J. Bishop-Moser, C. Kim, and S. Kota, “Kinematics of a Generalized Class of Pneumatic Artificial Muscles,” *J. Mechanisms Robotics*, vol. 7, no. 4, pp. 041014, 2015.
- [5] D. Bruder, A. Sedal, J. Bishop-Moser, S. Kota, and R. Vasudevan, “Model based control of fiber reinforced elastofluidic enclosures,” in *IEEE Int. Conf. on Robotics and Automation (ICRA)*, p. 5539-5544, 2017.
- [6] A. Sedal, D. Bruder, J. Bishop-Moser, R. Vasudevan, and S. Kota, “A Continuum Model for Fiber-Reinforced Soft Robot Actuators,” *J. Mechanisms and Robotics*, vol. 10, no. 2, pp. 024501, 2018.
- [7] D. Bruder, A. Sedal, R. Vasudevan, and C. D. Remy, “Force Generation by Parallel Combinations of Fiber-Reinforced Fluid-Drive Actuators,” in *2018 Int. Conf. Intelligent Robotics and Systems (IROS)*, Madrid, Spain.
- [8] A. Garriga-Casanovas, I. Collison, and F.R.Y. Baena, “Toward a Common Framework for the Design of Soft Robotic Manipulators with Fluidic Actuation,” *Soft Robotics*, published online: 30 Aug 2018 <https://doi.org/10.1089/soro.2017.0105>.
- [9] A. Sedal, A. Wineman, R. B. Gillespie, and C. D. Remy, “Comparison and Experimental Validation of Predictive Models for Soft, Fiber-Reinforced Actuators,” *Int. J. Robotics Research*, In press (*arXiv preprint arXiv:1902.00054*) 2019.
- [10] G. K. Klute, and B. Hannaford, “Accounting for Elastic Energy Storage in McKibben Artificial Muscle Actuators,” *J. Dyn. Sys., Meas., Control*, vol. 122, no. 2, pp. 386-388, 1998.
- [11] Natural Latex Rubber Tubing, New Age Industries, Retrieved from http://www.newageindustries.com/downloads/catalogs/NewAge_Rubber_Catalog.pdf, 2018.
- [12] A. N. Gent, “On the relation between indentation hardness and Young’s modulus,” *Rubber Chemistry and Technology*, vol. 31, no. 4, pp. 896-906, 1958.
- [13] D. Roylance, “Pressure Vessels,” Course notes, Dept. Mat. Sci. and Eng., M.I.T., Cambridge, MA, 2001.
- [14] G. A. Holzapfel, *Nonlinear Solid Mechanics*. West Sussex, England: Wiley, 2010, pp. 241-242.
- [15] H. Demirkoparan and T.J. Pence, “Magic angles for fiber reinforcement in rubber-elastic tubes subject to pressure and swelling,” *Int. J. Non-Linear Mech.*, vol. 68, pp. 87-95, 2015.